Antiviral Research 164 (2019) 123–130

Contents lists available at ScienceDirect

Antiviral Research

journal homepage: www.elsevier.com/locate/antiviral

GAP31 from an ancient medicinal plant exhibits anti-viral activity through targeting to Epstein-Barr virus nuclear antigen 1

Chih-Lung Shen[a,1], Wei-Han Huang[b,1], Hao-Jen Hsu[c], Jen-Hone Yang[d], Chih-Wen Peng[a,c,*]

[a] Institute of Medical Sciences, Tzu Chi University, Hualien, Taiwan
[b] Department of Oncology and Hematology, Buddhist Hualien Tzu Chi General Hospital, Hualien, Taiwan
[c] Department of Life Sciences, Tzu Chi University, Hualien, 97004, Taiwan
[d] College of Medicine, Tzu Chi University, Department of Dermatology, Buddhist Hualien Tzu Chi General Hospital, Hualien, Taiwan

ARTICLE INFO

Keywords:
Gelonium Anti-HIV Protein 31 kDa (GAP31)
Epstein-Barr virus (EBV)
EBV nuclear antigen 1 (EBNA1)
Latent replication origin (oriP)

ABSTRACT

Since it was discovered as the first human tumor virus in 1964, Epstein-Barr Virus (EBV) is now implicated in several types of malignancies. Accordingly, certain aspects of EBV pathobiology have shown promise in anti-cancer research in developing virus-targeting methods for EBV-associated cancers. The unique role of EBV nuclear antigen 1 (EBNA1) in triggering episome-dependent functions has made it as the only latent gene to be expressed in most EBV+ neoplasms. Dimeric EBNA1 binds to the replication origin (oriP) to display its biological impact on EBV-driven cell transformation and maintenance. Hence, EBNA1/oriP has been made an ideal drug target site for anti-EBV protocol development. GAP31 protein was originally isolated from the seeds of an ancient medicinal plant *Gelonium multiflorum*. Although GAP31 has been shown to exhibit both anti-viral and anti-tumor activity, current understanding of the mechanistic picture underlying GAP31 functioning is not clear. Herein, we identify the EBNA1 DNA-binding domain as a core for GAP31 binding by performing affinity pull-down assays. Recombinant GAP31 (rGAP31) was shown to impair EBNA1-induced dimerization; consequently, it abrogated both EBNA1/oriP-mediated binding and transcription. Importantly, the therapeutic effects of GAP31 showed its capability to abrogate EBV-driven cell transformation and proliferation, and EBV-dependent tumorigenesis in xenograft animal models. Notably, the EBNA1 binding-mutant $rGAP31_{R166A/R169A}$ simply exhibits defective phenotypes in the above-mentioned studies. Our data suggest rGAP31 is a potential anti-viral drug which can be applied to the development of therapeutic strategies against EBV-related malignancies.

1. Introduction

Epstein-Barr virus (EBV) is one of the most common human viruses that prevalently infect the adult population worldwide. The oncolytic potential of EBV has led to its causal links to several types of human lymphotropic and epitheliotropic neoplasms (Elgui de Oliveira et al., 2016). Transformation of B cells by EBV *in vitro* provides an assisted model system to study virus-induced pathogenesis and tumorigenesis (Liu et al., 2012; Roychowdhury et al., 2004). EBV-driven cell proliferation of B lymphocytes depends on a specific set of latency-associated nuclear antigens (EBNA), integral membrane proteins (LMPs), and non-coding RNAs (Longnecker et al., 2013). Among viral latent genes, only nuclear antigen 1 (EBNA1) is expressed in nearly all EBV + neoplastic cells, while others are restricted to distinct types of disorders, resulting into three classical latency-associated expressing patterns (Price and Luftig, 2015; Reedman and Klein, 1973). EBNA1 displays a diverse functional profile to support EBV persistence in host cells via binding to the cognate elements residing within the latent replication origin (oriP), including episome maintenance, viral and cellular transcription, and cell proliferation (Frappier, 2015). The EBNA1-DNA binding domain (DBD) induces dimerization when bound to oriP (Bochkarev et al., 1996; Frappier and O'Donnell, 1991); subsequently, it promotes the formation of a stable pre-initiating complex to couple with cellular factors to activate downstream events (Frappier, 2012a, b; Frappier et al., 1994).

Although it has been more than fifty years since the discovery of EBV, there is still no specific anti-viral drug for treating EBV-related cancers. The clinics mainly rely on the use of radiation and/or chemotherapy to treat EBV-associated malignancies; however, the presence of EBV frequently leads to poor prognosis (Leao et al., 2007; Shin et al., 2011; Song et al., 2005; Yoshimori et al., 2015). The fact that no EBNA1 ortholog has been identified implies a great specificity, and a reduction

* Corresponding author. Institute of Medical Sciences, Tzu-Chi University, 701 Zhong Yang Rd. Sec 3, Hualien 97004, Taiwan.
E-mail address: pengcw@mail.tcu.edu.tw (C.-W. Peng).
[1] These authors contribute equally in this work.

https://doi.org/10.1016/j.antiviral.2019.02.015
Received 25 September 2018; Received in revised form 12 January 2019; Accepted 22 February 2019
Available online 25 February 2019
0166-3542/

in side effects will be seen when EBNA1 inhibitors are applied for cancer therapy. In particular, inhibitors with the capability to interrupt EBNA1/oriP-dependent functions are conceptually considered as potential anti-EBV drugs (Chen et al., 2014, 2016; Sun et al., 2010; Thompson et al., 2010). Cumulative evidence supports that EBNA1 expression has a role in promoting metastasis and cancer cell proliferation (Frappier, 2015). The above features highlight the potential use of EBNA1 as the drug target for anti-EBV compound discovery.

The anti-viral protein, GAP31 (Gelonium Anti-HIV Protein, 31 kDa), which belongs to the family of ribosomal inactivation protein (RIP), was first known from the plant toxin gelonin and its novel anti-HIV activity was subsequently identified (Lee-Huang et al., 1991; Stirpe et al., 1980). GAP31 has been shown to elicit antiviral activities against HIV integration and Herpes simplex virus 1 (HSV1) infection (Bourinbaiar and Lee-Huang, 1996; Lee-Huang et al., 1995). Nevertheless, the mechanisms underlying GAP31-mediated antiviral response remain unknown. In addition to eliciting potent anti-tumor activity in cell-based studies, GAP31 also effectively debilitates tumorigenesis induced by xenograft breast cancer cells in SCID mice (Lee-Huang et al., 2000; Rybak et al., 1994).

The capability of GAP31 to selectively target virus-infected cells or tumor cells has highlighted a potential application of this protein in medical use. Nevertheless, the mechanistic insights underlying GAP31 functioning requires further explanation. In this study, we identify the specific binding of GAP31/EBNA1 and the potent anti-EBV activity of GAP31 is intensively characterized using cell-based studies and tumor xenograft mouse models.

2. Materials and methods

2.1. Expression plasmids, mutagenesis, and recombinant protein production

The synthetic cDNA of GAP31 (Genomics Inc, Taiwan) was used as the template for PCR. The DNA fragments encompassing the flanking sequences of GAP31 were subcloned into the *BamH*I and *Xho*I sites of the N-terminal Flag-epitope-tagged expression vector pSG5-Flag (Peng et al., 2004), or the *BamH*I and *Eco*RI sites of the bacterial expression vectors pGEX2TK (GE health care) and pTrcHisA (Thermo Fisher Scientific), respectively. The selected GAP31 or FEBNA1 mutants were generated using PCR mutagenesis kit (New England BioLabs). The EBNA1 derivative plasmids for bimolecular fluorescence complementation assay (BiFC) and the production of His-tagged or Glutathione S-transferases (GST)-fused GAP31 recombinant proteins were described previously (Chen et al., 2014; Peng et al., 2004).

2.2. Cell lines, cell culture, and EBV infection

BJAB is a B lymphoma cell line (Takimoto et al., 1986), AKATA(+) and AKATA(−) are Burkitt's lymphoma cell lines with EBV or without EBV infection (Takada et al., 1991). Lymphoblastoid cell lines (LCLs) are the resulting products from *in vitro* EBV mediated transformation of B cells. 293T is the derivative of human embryonic kidney 293 cells containing the SV40 T-antigen. The experimental procedures for primary B cells isolation, virus infection, cell culture, and EBV infection have been described previously (Shen et al., 2016).

2.3. Cell transfection and luciferase activity reporter assays

The protocol for cell transfection-mediated EBNA1-dependent transcription assays was described previously (Shen et al., 2016). In a cell-based reporter assay, 10^7 BJAB cells were co-transfected with 10 μg of the FEBNA1 expression vector, 5 μg of oriP-Luc reporter plasmid, and 1 μg of CMV-β Gal internal control plasmid, or 100 ng of GAP31/or mutant expression vector. In the control group, 10 μg of the EBNA2 expression vector, 5 μg of LMP1-Luc reporter plasmid, and 1 μg of CMV-β Gal internal control plasmid were used for transfection. When recombinant GAP31 proteins were applied, each transfectant was treated with indicated amounts of His-tagged GAP31 (rGAP31)/or E166A/R169A mutant (rGAP31m) for 16 h before the luciferase assay was conducted. Fold activation produced by each transfectant was determined as the luciferase activity corrected by the β-Gal activity. For 293T cells, the calcium phosphate transfection protocol was employed (Jordan et al., 1996).

2.4. Protein binding, DSS crosslinking, and immune blot analyses

GST, GST-GAP31 (gGAP31), or GST-GAP31m (gGAP31m) was mixed with cell lysates expressing FEBNA1 followed by an M2 (flag epitope)-conjugated sepharose mediated immunoprecipitation procedure. In the GST pulldown assay, gGAP31/or gGAP31m was used as the bait protein to pull down cell lysates expressing FEBNA1/or mutant derivatives, or EBNA2. For studying EBNA1-mediated homotypic interaction, eGFP, EBNA1 and FEBNA1 were co-transfected into BJAB cells with the treatments of selected amounts of rGAP31 or rGAP3m followed by immunoprecipitation using M2-sepharose beads. To access EBNA1 mediated dimerization, FEBNA1-expressing cell lysates were pretreated with GST, rGAP31, or rGAP31m for 2 h followed by 2 h of crosslinking using 1 mM disuccinimidyl suberate (DSS) prior to performing M2-flag immune-precipitation. The streptavidin agarose-mediated pulldown assay has been described previously (Chen et al., 2014). Antibodies for Flag-epitope M2 antibody (F3165; Sigma), GST (B14; Santa Cruz), His-tag (HIS.H8; Merck Millipore), EBNA1 (6F9/60; Novus Biologicals), EBNA2 (MABE8: Merck Millipore), Actin (C4; Santa Cruz) and GAPDH (2D4A7; Novus Biologicals) were used for immune blot analysis.

2.5. Long-term cell viability and BiFC assays

Cells were plated in duplicate in 24-well plates at a density of 5×10^3/0.5 mL in 24-well plates with increasing amounts of rGAP31 or rGAP31m treatment for 15 days. The medium was refreshed and replenished every three days with the same supplements. Cell numbers were counted every three days using Cellometer Vision CBA (Nexcelom). The BiFC signal was determined as % of fluorescent cells from the transfected population using above Cellometer.

2.6. Tumor xenograft studies, intratumoral injections, and immunohistochemistry (IHC)

Cells derived from LCL1 were used to prepare inoculums (5×10^5/100 μl) for a tumor xenograft study. Inoculums were treated with the selected concentrations of each recombinant protein for 72 h before subcutaneous (SC) injection was done. Six-week-old female NOD-SCID mice (Tzu Chi University Laboratory Animal Center) were used for SC injection into lower abdominal quadrants. The tumor sizes were calculated using the formulation $V = (L \times W^2)/2$, where V is the tumor volume, W is the tumor width, and L is the tumor length. Intratumoral injections using rGAP31/or rGAP31m were done twice a week from four to six post-weeks of tumor cell injection (pwi). The xenograft tumors produced in NOD SCID mice remained slightly different in size (total volume); thus we first calculated each tumor size independently. We then prepared the same volume of rGAP31 for each tumor before performing intratumoral injections. By doing so, we ensured that the amount of injected rGAP31 versus tumor volume was maintained at a constant ratio of 1:1. This experimental design allowed the injected rGAP31 to elicit almost the same effects to the tumors with varied sizes. All animal experiments were conducted under a protocol approved by the Tzu Chi University Institutional Animal Care and Use Committee. Xenograft tumor samples were isolated and fixed with 4% paraformaldehyde and subjected for an IHC-paraffin protocol using EBNA1 specific antibody (Abcam).

2.7. Statistical analysis

All statistical data were expressed as the mean ± standard deviation. Whenever necessary, statistical significance was determined by Student's *t*-test with P value < 0.05 (*), whereas P value > 0.05 (┼) means that no effect was observed.

3. Results

3.1. GAP31 down-regulates EBNA1/oriP-mediated transcription

Although both antiviral and antitumor activities of GAP31 have been documented in several studies, it remains unknown whether GAP31 has anti-EBV activity. Two well-established plasmid-mediated reporter systems were first used to rapidly screen the potential effects of GAP31 on either EBNA1-or EBNA2-dependent transcription of luciferase (Harter et al., 2016; Shen et al., 2016). GAP31 is a member of the RIP family, which is known to possess three conserved motifs within the protein context (Moghadam et al., 2016). Each codon of the selected conserved residues, Y74 (Motif I), Y113, E166/R169 (Motif II), and W198 (Motif III) was replaced by the alanine codon to generate four GAP31-derived expression plasmids, designated Y74A, Y113A, E166A/R169A, and W198A, respectively (sFig. 1A). The above plasmids were first used to assess their effects on either EBNA1/oriP-Luc or EBNA2/LMP1-Luc-mediated transcription in a cell-based transfection platform. Among GAP31 variants, transfected Y74A or W198A inhibited 50–70% of EBNA1/oriP-Luc-mediated transcription while Y113A and E166A/R169A had no effect (sFig. 1B). None of the GAP31-derived plasmids affected EBNA2/LMP1-Luc dependent transcription (sFig. 1C). As it only requires 100 ng of transfected GAP31 plasmid to produce robust effects on EBNA1/oriP-Luc-mediated transcription, such plasmid-expressed GAP31 is below the detectable limits by Western blot analysis. We next used recombinant GAP31 proteins, rGAP31 and GAP31m, to confirm the above findings (Fig. 1A). Treatments with 0.08–0.32 nm rGAP31 caused a 30%–80% reduction of EBNA/oriP-Luc induced transcription, whereas rGAP31m had no effect (Fig. 1B). In addition, neither rGAP31 nor rGAP31m exhibited potent inhibition to EBNA2/LMP1-Luc mediated transcription (Fig. 1C). Altogether, our data suggest GAP31 has specific effects on EBNA1/oriP-dependent functions.

3.2. Both EBNA1 DBD and GA domains are important for GAP31 binding

The observed repressive effects of GAP31 on EBNA1/oriP-Luc mediated transcription inspired us to explore whether GAP31/EBNA1 is linked via protein-protein interactions by performing protein pulldown assays (Fig. 2A). First, similar amounts of GST, gGAP31, or gGAP31m were used as bait proteins to pull down endogenous EBNA1 from an LCL. Approximately 0.5% of EBNA1 was rGAP31-bound while rGAP31m-bound EBNA1 was largely reduced to ~0.1% (Fig. 2A). GST did not appear to interact with EBNA1 and none of the above bait proteins was EBNA2-bound. In another set of protein-binding assays, we showed that the M2-Flag epitope (for FEBNA1) precipitated about 0.5% of gGAP31 and a slightly low amount of gGAP32m, whereas GST was not FEBNA1-bound (Fig. 2B–C). Advanced analysis showed that the deletion mutant of a glycine alanine-rich domain (aa. 90-325), ΔGA, completely lost gGAP31 binding, whereas ΔIM (387-459) remained gGAP31 bound (Fig. 2D). The C-terminal DBD is known to mediate EBNA1 homotypic interaction, thus cells with transfected FEBNA1, ΔDBD, or DBD were further used for the GST pulldown assay. The gGAP31 exhibited genuine protein interaction to FEBNA1 or DBD while it lost the capability to bind ΔDBD (Fig. 2E). Although DBD alone supported a low degree of binding to rGAP31, it required GA to maintain the interaction with rGAP31 in the context of whole EBNA1 protein. Moreover, the protein binding of gGAP31m to FEBNA1 or DBD was also identified while it was largely reduced to less than 10% of gGAP31's intrinsic binding activity. Altogether, our data indicate that both DBD and GA are important for binding to rGAP31.

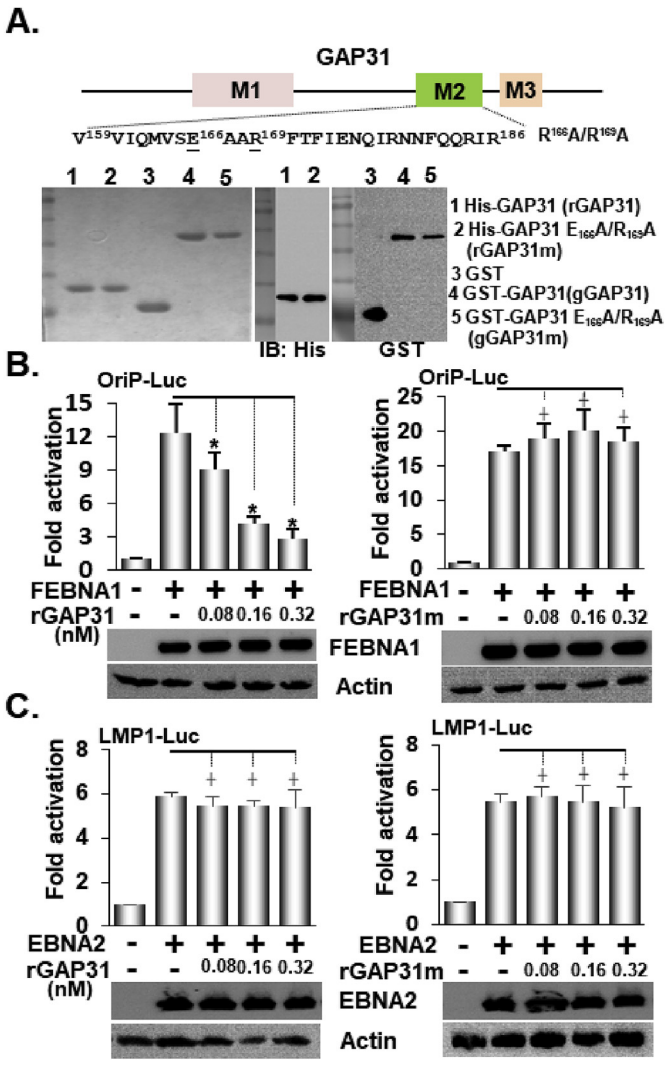

Fig. 1. rGAP31 impedes EBNA1/oriP-mediated transcription. (**A**) Affinity purification of His-tagged or GST-fused GAP31 and GAP31m. The purified proteins were verified by coomassie blue staining (left), and Western blot using His-tagged epitope (middle) or GST specific antibody (right). (**B**) BJAB cells transfected with FEBNA1 expression vector, oriP-Luc reporter plasmid, and β-Gal internal control were treated with indicated amounts of rGAP31 or rGAP31m for 24 h followed by a luciferase activity assay. The immune blots for FEBAN1 and actin were shown. For here and all following studies, representative p < 0.05(*) indicates significant differences between rGAP31-treated and control group, whereas p > 0.05(┼) means that no effect was observed. (**C**) The same above protocol was performed with the use of the EBNA2 expression vector and the LMP1-Luc reporter plasmid.

3.3. Blocking of EBNA1-mediated dimerization by GAP31 leads to abrogation of EBNA1/oriP binding

According to EBNA1-DBD-mediated dimerization, which is a general requirement for EBNA1/oriP-dependent functions (Bochkarev et al., 1996; Frappier, 2012a), we next explored whether GAP31 affects EBNA1 dimer formation. DSS mediated cross-linking of intracellularly expressed FEBNA1 was done after the pretreatments of rGAP31, rGAP31m, or GST. Without DSS, immune-precipitated FEBNA1 appeared in a monomeric format when it was resolved by SDS-PAGE and immune blot, whereas only dimeric FEBNA1 was observed when the cross-linking was done (Fig. 3A–B). Pretreatments with rGAP31 from 0.04 to 0.64 nm caused increasing degrees of FEBNA1 dissociation from

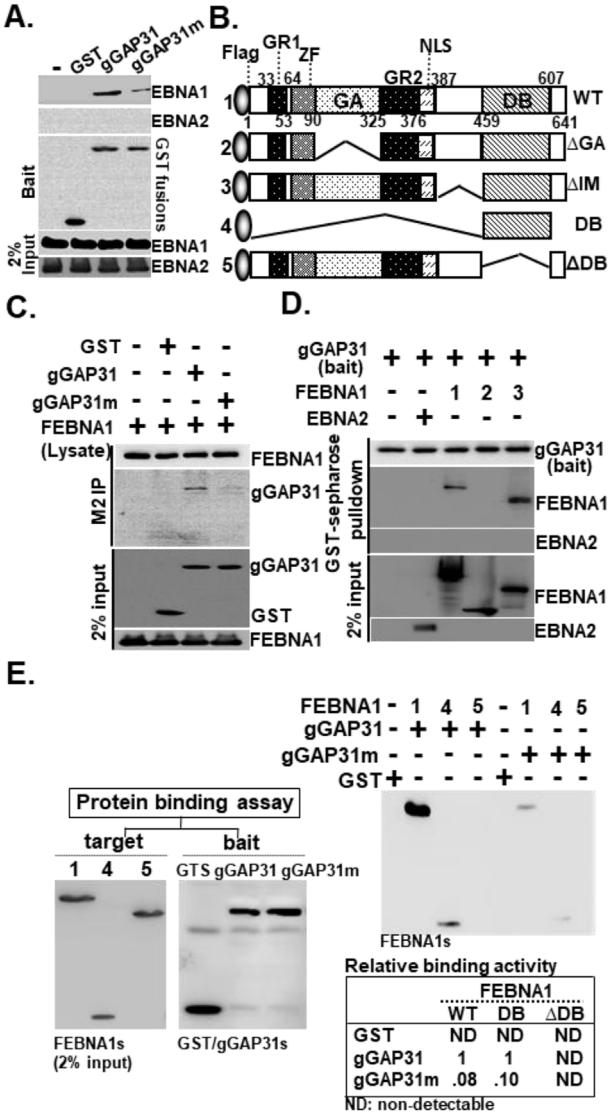

Fig. 2. Both EBNA1 GA and DBD domains are important for GAP31 binding. (**A**) GST, gGAP31, or gGAP31m was used as bait proteins to pulldown cell lysates from an LCL. The immune blot for the precipitated proteins and bait proteins were shown. 2% input of each target protein was shown. (**B**) Schematic diagrams of FEBNA1 and its mutant derivatives. (**C**) GST, gGAP31, or gGAP31m was mixed with FEBNA1 expressed cell lysates and subjected for M2-sepharose mediated immunoprecipitation assay. The immune blots for 2% input and co-precipitated proteins were shown (**D**) gGAP31 bound agaroses were used to pull down FEBNA1, its mutant derivative, or EBNA2 (control) from cell lysates. The amounts of bait, co-precipitated, or input proteins were identified by Western blot. (**E**) GST, gGAP31, or gGAP31m was used as a bait protein to pull down plasmid expressed FEBNA1, DBD, and ΔDBD from the transfected cell lysates, respectively. 2% input of EBNA1 was shown. The relative binding activity of each prey (FEBNA1 or its mutant derivatives) to bait (GST or GST-GAP31 fusions) proteins was verified by Western blot and quantified by Image J.

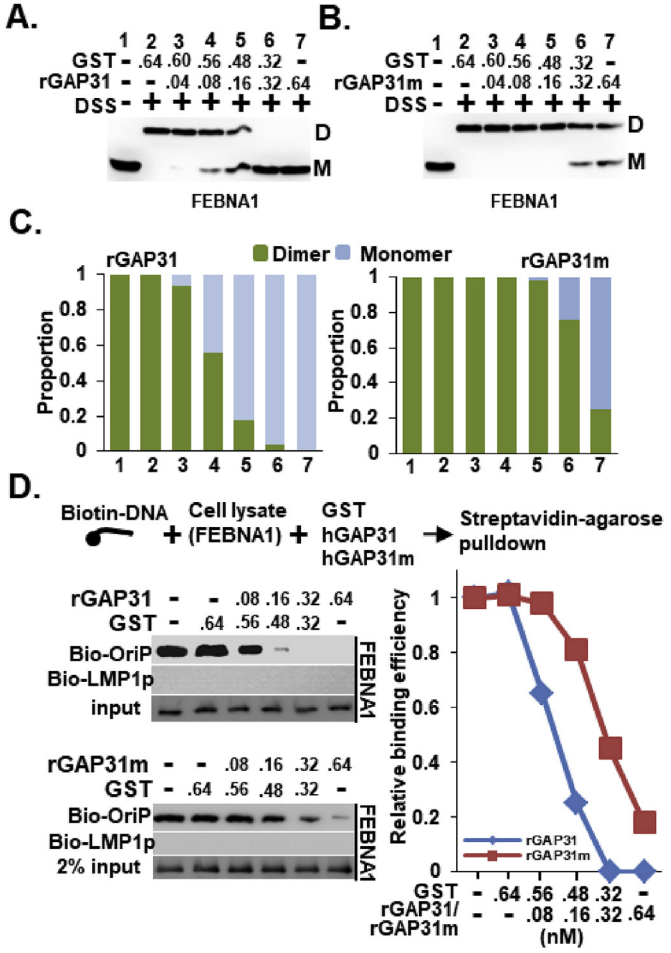

Fig. 3. GAP31 impairs EBNA1 dimer formation and EBNA1/oriP binding. (**A**) Cell lysates from FEBNA1 stably expressed BJAB cells were treated with indicated amounts of GST, gGAP31, or (**B**) gGAP31m followed by a DSS cross-linker protocol. FEBNA1 was immunoprecipitated by M2-sepharose. Monomeric or dimeric FEBNA1 was identified by Western blot. D:dimer versus M:monomer. (**C**) The proportion of EBNA1 dimer versus monomer in each sample was shown. (**D**) Bio-oriP or Bio-LMP1p was mixed with FEBNA1 expressed lysates treated with 0.64 nM GST or indicated amounts of rGAP31 or rGAP31m. Streptavidin-conjugated agaroses were used to precipitate above biotin-labeled DNA. The amounts of DNA bound FEBNA1 was determined by immune blot analysis and quantified by Image J.

the dimeric complex by 5%–100%, whereas 0.32 and 0.64 nm rGAP31m blocked ~20% and ~70% of FEBNA1-induced dimerization (Fig. 3C). In contrast, 0.04–0.16 nM rGAP31m had no blocking activity. In the co-immunoprecipitation assay, 0.32 nM rGAP31 completely blocked the homotypic interaction mediated by FEBNA1/EGFP-EBNA1 while the same dose of rGAP31m only exhibited 50% blocking activity of rGAP31 (sFig. 2A). The *in vivo* effects of rGAP31 on EBNA1 homotypic interaction were next monitored by a BiFC assay. Treatments with rGAP31 by 0.08, 0.16, and 0.32 nM caused 55%, 78%, and 82% reduction of the BiFC signal, whereas the same treatments of rGAP31m caused BiFC reduction by 7%, 23% and 42% (sFig. 2B). In the control group, we showed EBNA2-induced BiFC was barely impaired by 0.08–0.32 nM rGAP31, resulting in a ~1–~10% reduction of the BiFC signal (sFig. 2C). Taken together, the three different protein-oligomerization analytic platforms confirm that GAP31 is indeed an antagonist for EBNA1-mediated dimerization.

Given the maintenance of EBNA1-dimer is directly linked to EBNA1/oriP binding, a streptavidin-agarose pulldown assay was next employed to evaluate the blocking effects of GAP31 to the above event (Chen et al., 2014). Treatments by rGAP31 from 0.08 to 0.32 nM were inhibited by 30%–100% while rGAP31m from 0.08 to 0.64 nM resulted a 5%–80% reduction of FEBNA1 binding to the biotin-labeled oriP-DNA (bio-oriP)(Fig. 3D). In contrast, 0.64 nM GST had no blocking effect. The Biotin-labeled LMP1-promoter (Bio-LMP1p) did not show any binding potency to FEBNA1. Our data demonstrate that the inhibitory effects of GAP31 to EBNA1 dimerization readily lead to interruption of downstream EBNA1/oriP binding.

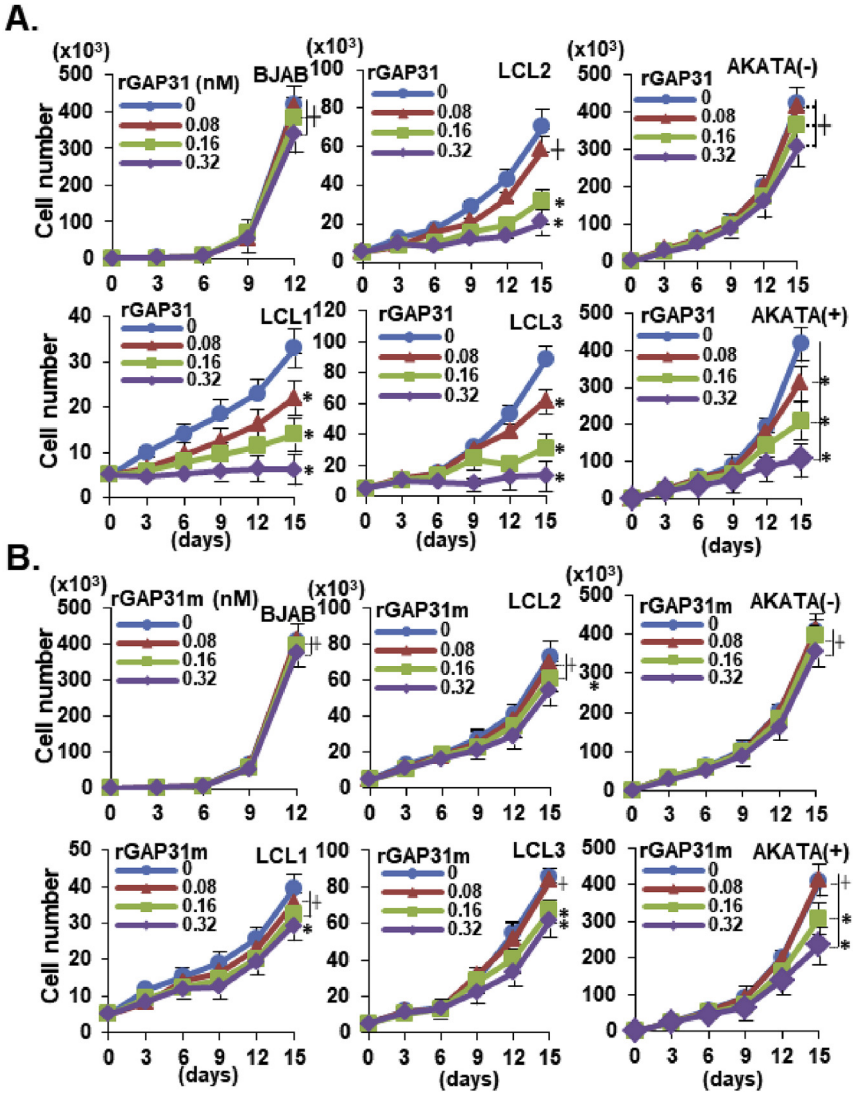

Fig. 4. GAP31 debilitates EBV dependent cell growth. (**A**) The cell proliferation assay was conducted using three LCLs (LCL1-3), BJAB B lymphoma cells, and two Burkitt's lymphoma cell lines: AKATA(+) vs. AKATA(−). Equal numbers (5×10^3/0.5 mL) of cells were seeded in 24-well plates with the treatments of rGAP31 from 0 to 0.32 nM. Cell numbers were counted every three days. (**B**) The same cell proliferation assay was performed except the rGAP31 was replaced by rGAP31m.

3.4. rGAP31 impairs EBV-driven cell proliferation

The blocking effects of GAP31 to EBNA1/oriP-dependent functions are expected to impair EBV-driven cell proliferation. Along with this line, three LCLs, EBV-negative BJAB B lymphoma cells, Burkitt's Lymphoma-derived EBV positive AKATA(+), and EBV-negative AKATA(−) cells with the treatments of 0.08–0.32 nM GAP31 or rGAP31m were subjected to cell proliferation assays. The rGAP31 caused similar defective phenotypes in three LCLs and AKATA(EBV+) cells (Fig. 4A). The 0.08 nM rGAP31 was partially impaired while 0.16 and 0.32 nM rGAP31 caused approximately 70% and 90% reduction of cell proliferation by day 15. Notably, rGAP31 from 0.08 to 0.32 nM had either none or minor effects to BJAB and AKATA(−) cells. The rGAP31m had limited influence on cell growth of LCL3 or AKATA(+) when 0.16 or 0.32 nM was applied, whereas all of the selected doses did not change the proliferating patterns of other cell lines (Fig. 4B).

3.5. rGAP31 elicits robust anti-viral activity against EBV-mediated cell transformation and tumorigenesis

The potent EBNA1-targeting activity of GAP31 was next validated for its effects on EBV- mediated transformation and tumorigenesis. In an *in vitro* EBV-driven B cell transformation assay, 0.08 and 0.32 nM rGAP31 inhibited ~30% and ~60% EBV-driven transformation outgrowth by 18 days of post-infection (dpi), whereas the above event was completely abrogated by 0.64 nM rGAP31. The rGAP31m impaired ~30% of EBV-induced outgrowth at 0.64 nM while it only produced barely detectable blocking activity when 0.08–0.32 nM was used. In the absence of EBV infection, no rGAP31/or rGAP31m treatments caused deleterious effects on the maintenance of primary B cells (sFig. 3A).

Given LCLs were shown as good material sources for studying EBV-induced tumorigenesis [(Roychowdhury et al., 2004) and Fig. 5B], the anti-cancer activity of GAP31 was evaluated using the tumor xenograft NOD/SCID mouse model. LCL-derived xenograft tumors firstly appeared at approximately 4 pwi, which were verified by their expression of three EBV-latent genes (EBNA1, EBNA2, and LMP1) and by EBNA1 IHC staining (Fig. 5C). According to the treatments of rGAP31 or rGAP31m from 0.08 to 0.64 nM did not impair LCL growth by three days (Fig. 4A), cells pretreated with GST control, rGAP31, or rGAP31m for 72 h were utilized for SC injection. Surprisingly, all LCL inoculums with pretreatments of rGAP31 from 0.08 to 0.64 nM failed to produce xenograft tumors (sFig. 3B). Tumor sizes were gradually reduced from 0.85 to 0.3 cm^3 at eight pwi when LCL inoculums were pretreated with 0.08–064 nM rGAP31m (sFig. 3C). The anti-tumor activity of rGAP31

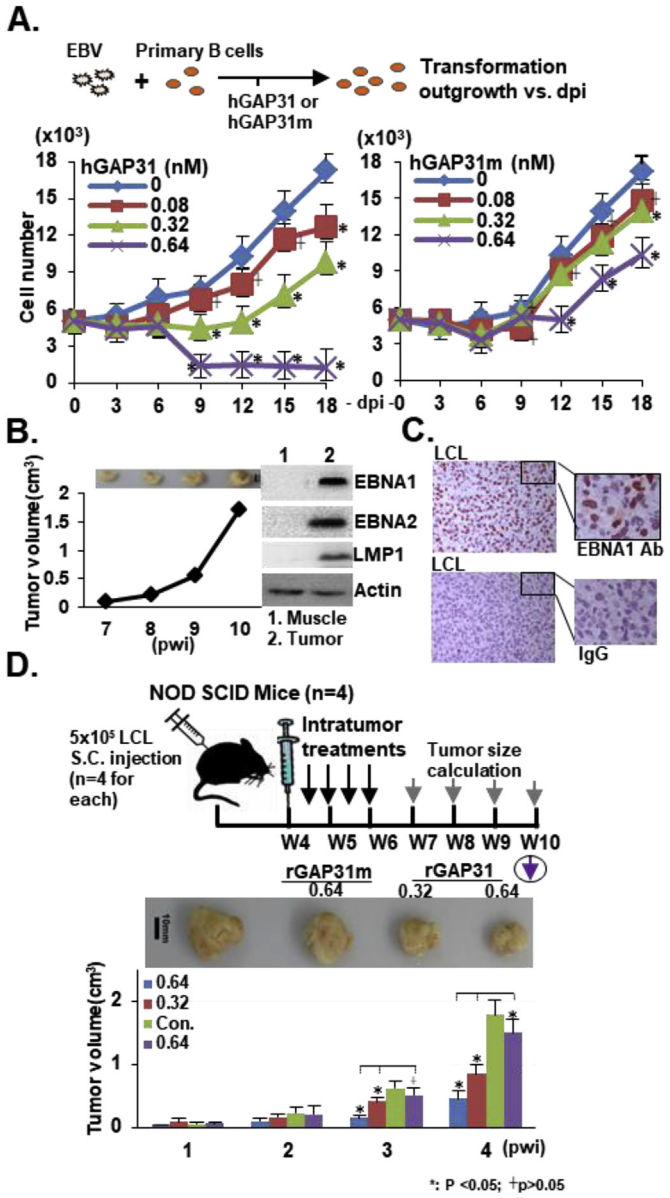

Fig. 5. GAP31 blocks EBV-mediated transformation and EBV-induced tumorigenesis. (**A**) Primary B cells with the treatments of rGAP31 (left) or rGAP31m (right) from 0.08 to 0.64 were used for EBV mediated transformation outgrowth. EBV driven B cell proliferation was monitored from 0 to 18 dpi. (**B**) NOD-SCID mice were subcutaneously injected with LCL1, xenograft tumors were calculated and isolated from mice weekly from seven to ten pwi. (**C**) Solid tumors were isolated and applied for IHC analysis using EBNA1 specific antibody or IgG control. (**D**) Intratumoral injections with indicated amounts of rGAP31 or rGAP31m were performed twice per week from four to six pwi. Tumor sizes were calculated weekly from seven to ten pwi. Tumors were isolated at ten pwi and examined.

was further evaluated by intratumoral injection. LCL-induced solid tumors were injected with indicated amounts of the GST control (a total of five injections), GAP31, or rGAP31m twice a week from 4 to 6 pwi (Fig. 5D). Intratumoral treatments with 0.32 and 0.64 nM rGAP31 caused a reduction of tumor sizes from approximately 1.8 to 0.8 and 0.4 cm^3, whereas 0.64 nm rGAP31m simply caused ~10% reduction of tumor sizes by 10 pwi.

4. Discussion

Among the currently known human tumor viruses, EBV appears as a grant challenge in anti-cancer development because neither effective vaccines nor drugs are clinically available. The development of novel methods for either targeting EBV-latent or lytic proteins is an urgent medical need. Binding of EBNA1 dimers to the cognate element is a prerequisite for EBNA1/oriP-dependent functions (Ceccarelli and Frappier, 2000), thus inhibition of EBNA1-mediated dimerization or blocking of EBNA1/oriP binding should lead to virtual cleaning out of EBV from host cells. The high throughput screening platforms for small molecules or organic compounds in anti-EBNA1 drug discovery reflect a great potential of using virus-targeting strategies to fight against EBV-related diseases (Choi et al., 2015; Gianti et al., 2016; Li et al., 2010b).

Apart from its ribosomal inactivation functions, RIPs catch most attraction for their use in antibacterial, antifungal, anti-cancer, and anti-virus research (Stirpe, 2013; Zhu et al., 2018). Currently, RIPs are divided into three major categories, type I to III, according to their physical property (Zhu et al., 2018). RIPs have been shown to elicit potent anti-cancer activity, primarily dependent on their capability to induce apoptosis in a variety of cancer cells (Zeng et al., 2015). Nevertheless, the mechanistic insight of RIP-mediated anti-viral response is largely unknown. The members of type I RIP, GAP31, and MAP30 (Momordica anti-HIV protein of 30 kDa), have been shown to exhibit inhibition of HIV-1 integrase via their intrinsic DNA glycosidase activity (Lee-Huang et al., 1995; Li et al., 2010a). The apparent lack of a lectin-like B chain moiety in type I RIPs is expected to produce lower toxicity than Type II RIPs due to poor entry capability. The use of a 100 ng-transfected GAP31 plasmid DNA can cause a 60% reduction of EBNA1/oriP-Luc-mediated transcription, indicating an extremely low dose of the compound is sufficient to elicit EBNA1-targeting activity as soon as it is introduced into cells. The EBNA1 targeting potency of rGAP31 further highlights its application in EBV associated malignancies. The EBNA1 dependence proliferation of EBV+ AKATA cells has been well characterized (Sun et al., 2010). Since we did not observe any significant difference in cell proliferation for EBV+ versus EBV- AKATA cells, the observed specific effects of rGAP31 on EBV+ AKATA versus EBV- AKATA cells are more likely due to its EBNA1 targeting activity.

Recent advances in structural analysis and molecular modeling revealed that the EBNA1-DBD binding mutant $GAP31_{E166A/R169A}$ is predicted to possess null DNA accessibility (Li et al., 2010a). The specific protein-protein interaction mediated by GAP31 and EBNA1-DBD is likely due to their innate structural features which are well-suited for DNA binding. Our findings suggest that RIPs may have evolved as a structurally-fitted moiety to associate with certain viral proteins possessing DNA binding features. The binding of GAP31 to monomeric EBNA1-DBD could ultimately change its conformation or occupy its docking site to prevent the binding from another EBNA1 molecule. Our study highlights a minimum use of rGAP31 by 0.32–0.64 nM is sufficient to shut down nearly all EBNA1/oriP-dependent functions. Of importance, these doses of rGAP31 ultimately produce robust biological impacts to block EBV-mediated transformation and tumorigenesis. The unique binding affinity of GAP31 to EBNA1-DBD and its low toxicity to virus-uninfected cells or normal cells are expected to immensely reduce undesired side effects (Bourinbaiar and Lee-Huang, 1996; Lee-Huang et al., 1995), implying a great potential to use GAP31 in anti-EBV drug development.

It should be noted that the direct use of rGAP31 in clinics may not be feasible since it remains unclear how rGAP31 mediates entry into cells. As we have demonstrated that rGAP31 only requires 0.32–0.64 nM to completely block EBNA1-dependent functions, this implies rGAP31 likely has evolved a specific strategy for cell targeting through recognizing receptors or surface proteins. By far, the working model of GAP31-mediated anti-viral response has been well-characterized in HIV. A GAP31 peptide with N-terminal 33 amino acids is sufficient for HIV inhibition (Lee-Huang et al., 1994), whereas our study suggested that GAP31 motif II is the critical module for EBNA1-blocking activity. It can be expected that GAP31-driven anti-viral

response is mechanistically different from virus to virus. Knowing GAP31-mediated protein binding to EBNA1 from a structural aspect will be a critical requirement prior to using rGAP31 for potential clinical use. If the minimum EBNA1-binding domain or short peptide can be identified, the above materials can be carried by nano-particles/or small molecules for the development of cell type-specific delivery tools. Of importance, knowing how to ensure those rGAP31 derived protein- or peptide-drugs can exhibit good EBV targeting activity after delivery into cells is a critical concern. With a proper design of the rGAP31 delivery complex for specific targeting, it will also reduce severe side effects caused by current use of chemotherapy in lymphomas.

Conflicts of interest

The authors declare that they do not have any commercial or associative interest that represents a conflict of interest in connection with the work submitted.

Grant support

The research work is supported by TCMMP105-07-01 and 106-03-01 from Buddhist Tzu Chi Medical Foundation Taiwan, and MOST 105-2320-B-320-013-MY3 and MOST 106-2320-B-320 -004 -MY3 from the Minister of Science and Technology Taiwan to C.W.P., TCMMP105-07-03 and 106-03-01 from Buddhist Tzu Chi Medical Foundation Taiwan to W.H.H., and MOST 105-2314-B-303-009-MY3 from the Minister of Science and Technology Taiwan to J.H.Y. The founder has no role in study design, data collection and analysis, decision to publish or preparation of the manuscript.

Acknowledgements

The authors acknowledge Ms Hsuen-Huei Wu for the assistance in GAP31 plasmid preparation.

Appendix A. Supplementary data

Supplementary data to this article can be found online at https://doi.org/10.1016/j.antiviral.2019.02.015.

References

Bochkarev, A., Barwell, J.A., Pfuetzner, R.A., Bochkareva, E., Frappier, L., Edwards, A.M., 1996. Crystal structure of the DNA-binding domain of the Epstein-Barr virus origin-binding protein, EBNA1, bound to DNA. Cell 84, 791–800.

Bourinbaiar, A.S., Lee-Huang, S., 1996. The activity of plant-derived antiretroviral proteins MAP30 and GAP31 against herpes simplex virus in vitro. Biochem. Biophys. Res. Commun. 219, 923–929.

Ceccarelli, D.F., Frappier, L., 2000. Functional analyses of the EBNA1 origin DNA binding protein of Epstein-Barr virus. J. Virol. 74, 4939–4948.

Chen, Y., Lu, Z., Zhang, L., Gao, L., Wang, N., Gao, X., Wang, Y., Li, K., Gao, Y., Cui, H., Gao, H., Liu, C., Zhang, Y., Qi, X., Wang, X., 2016. Ribosomal protein L4 interacts with viral protein VP3 and regulates the replication of infectious bursal disease virus. Virus Res. 211, 73–78.

Chen, Y.L., Liu, C.D., Cheng, C.P., Zhao, B., Hsu, H.J., Shen, C.L., Chiu, S.J., Kieff, E., Peng, C.W., 2014. Nucleolin is important for Epstein-Barr virus nuclear antigen 1-mediated episome binding, maintenance, and transcription. Proc. Natl. Acad. Sci. U. S. A. 111, 243–248.

Choi, C.K., Ho, D.N., Hui, K.F., Kao, R.Y., Chiang, A.K., 2015. Identification of Novel Small Organic Compounds with Diverse Structures for the Induction of Epstein-Barr Virus (EBV) Lytic Cycle in EBV-Positive Epithelial Malignancies. PLoS One 10, e0145994.

Elgui de Oliveira, D., Muller-Coan, B.G., Pagano, J.S., 2016. Viral carcinogenesis beyond malignant transformation: EBV in the progression of human cancers. Trends Microbiol. 24, 649–664.

Frappier, L., 2012a. Contributions of Epstein-Barr nuclear antigen 1 (EBNA1) to cell immortalization and survival. Viruses 4, 1537–1547.

Frappier, L., 2012b. EBNA1 and host factors in Epstein-Barr virus latent DNA replication. Curr. Opin. Virol. 2, 727–733.

Frappier, L., 2015. Ebna1. Curr. Top. Microbiol. Immunol. 391, 3–34.

Frappier, L., Goldsmith, K., Bendell, L., 1994. Stabilization of the EBNA1 protein on the Epstein-Barr virus latent origin of DNA replication by a DNA looping mechanism. J. Biol. Chem. 269, 1057–1062.

Frappier, L., O'Donnell, M., 1991. Epstein-Barr nuclear antigen 1 mediates a DNA loop within the latent replication origin of Epstein-Barr virus. Proc. Natl. Acad. Sci. U. S. A. 88, 10875–10879.

Gianti, E., Messick, T.E., Lieberman, P.M., Zauhar, R.J., 2016. Computational analysis of EBNA1 "druggability" suggests novel insights for Epstein-Barr virus inhibitor design. J. Comput. Aided Mol. Des. 30, 285–303.

Harter, M.R., Liu, C.D., Shen, C.L., Gonzalez-Hurtado, E., Zhang, Z.M., Xu, M., Martinez, E., Peng, C.W., Song, J., 2016. BS69/ZMYND11 C-Terminal Domains Bind and Inhibit EBNA2. PLoS Pathog. 12, e1005414.

Jordan, M., Schallhorn, A., Wurm, F.M., 1996. Transfecting mammalian cells: optimization of critical parameters affecting calcium-phosphate precipitate formation. Nucleic Acids Res. 24, 596–601.

Leao, M., Anderton, E., Wade, M., Meekings, K., Allday, M.J., 2007. Epstein-barr virus-induced resistance to drugs that activate the mitotic spindle assembly checkpoint in Burkitt's lymphoma cells. J. Virol. 81, 248–260.

Lee-Huang, S., Huang, P.L., Huang, P.L., Bourinbaiar, A.S., Chen, H.C., Kung, H.F., 1995. Inhibition of the integrase of human immunodeficiency virus (HIV) type 1 by anti-HIV plant proteins MAP30 and GAP31. Proc. Natl. Acad. Sci. U. S. A. 92, 8818–8822.

Lee-Huang, S., Huang, P.L., Sun, Y., Chen, H.C., Kung, H.F., Huang, P.L., Murphy, W.J., 2000. Inhibition of MDA-MB-231 human breast tumor xenografts and HER2 expression by anti-tumor agents GAP31 and MAP30. Anticancer Res. 20, 653–659.

Lee-Huang, S., Kung, H.F., Huang, P.L., Bourinbaiar, A.S., Morell, J.L., Brown, J.H., Huang, P.L., Tsai, W.P., Chen, A.Y., Huang, H.I., et al., 1994. Human immunodeficiency virus type 1 (HIV-1) inhibition, DNA-binding, RNA-binding, and ribosome inactivation activities in the N-terminal segments of the plant anti-HIV protein GAP31. Proc. Natl. Acad. Sci. U. S. A. 91, 12208–12212.

Lee-Huang, S., Kung, H.F., Huang, P.L., Huang, P.L., Li, B.Q., Huang, P., Huang, H.I., Chen, H.C., 1991. A new class of anti-HIV agents: GAP31, DAPs 30 and 32. FEBS Lett. 291, 139–144.

Li, H.G., Huang, P.L., Zhang, D., Sun, Y., Chen, H.C., Zhang, J., Huang, P.L., Kong, X.P., Lee-Huang, S., 2010a. A new activity of anti-HIV and anti-tumor protein GAP31: DNA adenosine glycosidase–structural and modeling insight into its functions. Biochem. Biophys. Res. Commun. 391, 340–345.

Li, N., Thompson, S., Schultz, D.C., Zhu, W., Jiang, H., Luo, C., Lieberman, P.M., 2010b. Discovery of selective inhibitors against EBNA1 via high throughput in silico virtual screening. PLoS One 5, e10126.

Liu, C.D., Chen, Y.L., Min, Y.L., Zhao, B., Cheng, C.P., Kang, M.S., Chiu, S.J., Kieff, E., Peng, C.W., 2012. The nuclear chaperone nucleophosmin escorts an Epstein-Barr Virus nuclear antigen to establish transcriptional cascades for latent infection in human B cells. PLoS Pathog. 8, e1003084.

Longnecker, R., Kieff, E., Cohen, J., 2013. Epstein-Barr virus. In: Knipe, D., Howley, P. (Eds.), Fields Virology, sixth ed. Lippincott, Williams, and WIlkins, Philadelphia, pp. 1898–1959.

Moghadam, A., Niazi, A., Afsharifar, A., Taghavi, S.M., 2016. Expression of a Recombinant Anti-HIV and Anti-Tumor Protein, MAP30, in Nicotiana tabacum Hairy Roots: a pH-Stable and Thermophilic Antimicrobial Protein. PLoS One 11, e0159653.

Peng, C.W., Xue, Y., Zhao, B., Johannsen, E., Kieff, E., Harada, S., 2004. Direct interactions between Epstein-Barr virus leader protein LP and the EBNA2 acidic domain underlie coordinate transcriptional regulation. Proc. Natl. Acad. Sci. U. S. A. 101, 1033–1038.

Price, A.M., Luftig, M.A., 2015. To be or not IIb: a multi-step process for Epstein-Barr virus latency establishment and consequences for B cell tumorigenesis. PLoS Pathog. 11, e1004656.

Reedman, B.M., Klein, G., 1973. Cellular localization of an Epstein-Barr virus (EBV)-associated complement-fixing antigen in producer and non-producer lymphoblastoid cell lines. Int. J. Cancer 11, 499–520.

Roychowdhury, S., Baiocchi, R.A., Vourganti, S., Bhatt, D., Blaser, B.W., Freud, A.G., Chou, J., Chen, C.S., Xiao, J.J., Parthun, M., Chan, K.K., Eisenbeis, C.F., Ferketich, A.K., Grever, M.R., Chen, C.S., Caligiuri, M.A., 2004. Selective efficacy of depsipeptide in a xenograft model of Epstein-Barr virus-positive lymphoproliferative disorder. J. Natl. Cancer Inst. 96, 1447–1457.

Rybak, S., Lin, J., Newton, D., Kung, H., Monks, A., Chen, H., Huang, P., Leehuang, S., 1994. In-vitro antitumor-activity of the plant ribosome-inactivating proteins map-30 and gap-31. Int. J. Oncol. 5, 1171–1176.

Shen, C.L., Liu, C.D., You, R.I., Ching, Y.H., Liang, J., Ke, L., Chen, Y.L., Chen, H.C., Hsu, H.J., Liou, J.W., Kieff, E., Peng, C.W., 2016. Ribosome protein L4 is essential for epstein-barr virus nuclear antigen 1 function. Proc. Natl. Acad. Sci. U. S. A. 113, 2229–2234.

Shin, H.J., Kim, D.N., Lee, S.K., 2011. Association between Epstein-Barr virus infection and chemoresistance to docetaxel in gastric carcinoma. Mol. Cells 32, 173–179.

Song, J.M., Lee, K.H., Seong, B.L., 2005. Antiviral effect of catechins in green tea on influenza virus. Antivir. Res. 68, 66–74.

Stirpe, F., 2013. Ribosome-inactivating proteins: from toxins to useful proteins. Toxicon 67, 12–16.

Stirpe, F., Olsnes, S., Pihl, A., 1980. Gelonin, a new inhibitor of protein synthesis, non-toxic to intact cells. Isolation, characterization, and preparation of cytotoxic complexes with concanavalin A. J. Biol. Chem. 255, 6947–6953.

Sun, X., Barlow, E.A., Ma, S., Hagemeier, S.R., Duellman, S.J., Burgess, R.R., Tellam, J., Khanna, R., Kenney, S.C., 2010. Hsp90 inhibitors block outgrowth of EBV-infected malignant cells in vitro and in vivo through an EBNA1-dependent mechanism. Proc. Natl. Acad. Sci. U. S. A. 107, 3146–3151.

Takada, K., Horinouchi, K., Ono, Y., Aya, T., Osato, T., Takahashi, M., Hayasaka, S., 1991. An Epstein-Barr virus-producer line Akata: establishment of the cell line and analysis of viral DNA. Virus Gene. 5, 147–156.

Takimoto, T., Sato, H., Ogura, H., 1986. Primary EBV infection of human umbilical cord lymphocytes and EBV genome-negative lymphoblastoid cell lines (BJAB and Ramos).

Auris Nasus Larynx 13, 199–205.
Thompson, S., Messick, T., Schultz, D.C., Reichman, M., Lieberman, P.M., 2010. Development of a high-throughput screen for inhibitors of Epstein-Barr virus EBNA1. J. Biomol. Screen 15, 1107–1115.
Yoshimori, M., Takada, H., Imadome, K., Kurata, M., Yamamoto, K., Koyama, T., Shimizu, N., Fujiwara, S., Miura, O., Arai, A., 2015. P-glycoprotein is expressed and causes resistance to chemotherapy in EBV-positive T-cell lymphoproliferative diseases. Cancer Med. 4, 1494–1504.
Zeng, M., Zheng, M., Lu, D., Wang, J., Jiang, W., Sha, O., 2015. Anti-tumor activities and apoptotic mechanism of ribosome-inactivating proteins. Chin. J. Cancer 34, 325–334.
Zhu, F., Zhou, Y.K., Ji, Z.L., Chen, X.R., 2018. The plant ribosome-inactivating proteins play important roles in defense against pathogens and insect pest attacks. Front. Plant Sci. 9, 146.